Hydrogen Storage

DOI: 10.1002/anie.201100810

The Particle-Size Dependence of the Activation Energy for Decomposition of Lithium Amide**

*Khang Hoang, Anderson Janotti, and Chris G. Van de Walle**

Dedicated to the Fritz Haber Institute, Berlin, on the occasion of its 100th anniversary

Lithium amide ($LiNH_2$) is a promising material for reversible hydrogen storage,[1] yet the atomistic mechanisms behind the decomposition and dehydrogenation processes of $LiNH_2$ are unknown. It has been observed that the activation energy for $LiNH_2$ decomposition strongly varies with ball milling,[2–4] thus suggesting that the thermodynamics and kinetics of the decomposition depend on the particle size. The high surface-to-volume ratio of nanoparticles that result from the ball-milling process not only leads to an increase in the number of surface-active sites for reaction, but may also affect the actual reaction mechanisms. Based on results of ab initio calculations for native point defects and defect complexes in $LiNH_2$, we propose herein that the decomposition of $LiNH_2$ into lithium imide (Li_2NH) and ammonia (NH_3) occurs through two competing mechanisms, one that involves the formation of native defects in the interior of the material and the other at the surface. As a result, the prevailing mechanism and hence the activation energy depend on the surface-to-volume ratio, or the specific surface area (SSA), which changes with the particle size. We explain the observed variation of activation energy with ball milling, and address the role played by LiH in the dehydrogenation of ($LiNH_2$+LiH) mixtures.

At temperatures below 300 °C, $LiNH_2$ reversibly stores approximately 6.5 wt % hydrogen during absorption under 20 bar followed by desorption under 0.04 bar, according to the following reaction [Eq. (1)]:[1]

$$LiNH_2+LiH \leftrightarrow Li_2NH+H_2 \quad (1)$$

It has been suggested that $LiNH_2$ reacts directly with LiH at the $LiNH_2$/LiH interface, with direct release of H_2.[1] Other reports, however, proposed that NH_3 necessarily evolves as a transient gas and the dehydrogenation of ($LiNH_2$ + LiH) mixtures involves an intermediate step [Eqs. (2) and (3)]:[5,6]

$$2\,LiNH_2 \rightarrow Li_2NH+NH_3 \quad (2)$$

$$NH_3+LiH \rightarrow LiNH_2+H_2 \quad (3)$$

The first reaction [Eq. (2)] was suggested to be diffusion-controlled,[2,7] that is, involving mass transport mediated by native defects; whereas in the second reaction [Eq. (3)], NH_3 was reported to be readily captured by LiH at very short contact times (ca. 25 ms).[5] After ball milling, $LiNH_2$ and ($LiNH_2$+LiH) mixtures were found to have smaller particle size, increased specific surface area (SSA), and lower activation energy.[2–4]

$LiNH_2$ can be regarded as an ordered arrangement of Li^+ and NH_2^- units. Possible native point defects in the compound are vacancies, interstitials, and antisite defects associated with lithium, nitrogen, and hydrogen atoms. In insulating, large-band-gap materials such as $LiNH_2$, native point defects are expected to exist in charged states other than neutral, and charge neutrality requires that defects with opposite charge states coexist in equal concentrations. This requirement, and the fact that migration of charged defects has to maintain local and global charge neutrality, forms the basis of our analysis.

We carried out calculations for native defects in all possible charge states by using ab initio density functional theory. Defect complexes were also considered, with special attention to Frenkel pairs, that is, interstitial-vacancy pairs of the same species. The defects are characterized by their formation energies, which determine their concentrations, and migration barriers. The formation energy depends on the atomic chemical potentials, which can be chosen to represent the experimental conditions (see the technical details of the calculations and the theoretical approach in the Methods section). For charged defects, the formation energy also depends on the position of the Fermi level (i.e., the electron chemical potential). The slope in the formation-energy plots as a function of the Fermi level indicates the charge state. A positive slope indicates that the defect is positively charged, and a negative slope indicates the defect is negatively charged. We present the results only for selected defects that are most relevant to our present discussion. Detailed results for all possible native defects will be reported elsewhere.

Figure 1 shows the calculated formation energies for the negatively charged hydrogen vacancy (V_H^-), positively charged hydrogen interstitial (H_i^+), negatively charged lithium vacancy (V_{Li}^-), and positively charged lithium interstitial (Li_i^+). These defects have low formation energies and are, as discussed below, most relevant to the decomposition of $LiNH_2$. Li_i^+ and V_{Li}^- have the lowest formation energies

[*] Dr. K. Hoang, Dr. A. Janotti, Prof. C. G. Van de Walle
Materials Department, University of California
Santa Barbara, CA 93106 (USA)
E-mail: vandewalle@mrl.ucsb.edu
Homepage: http://www.mrl.ucsb.edu/~vandewalle

[**] K.H. was supported by General Motors Corporation, and A.J. by the U. S. Department of Energy (grant no. DE-FG02-07ER46434). We acknowledge use of the CNSI Computing Facility under NSF grant no. CHE-0321368 and NERSC resources supported by the DOE Office of Science under contract no. DE-AC02-05CH11231.

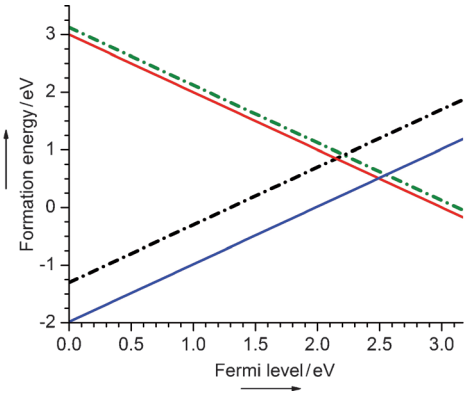

Figure 1. Calculated formation energies of selected native point defects in $LiNH_2$, plotted as a function of Fermi level with respect to the valence-band maximum (VBM). Li_i^+ (blue), V_{Li}^- (red), H_i^+ (black), and V_H^- (green). The calculated band gap of pristine $LiNH_2$ is 3.17 eV, from the VBM to the conduction-band minimum (CBM).

among all native point defects over the entire range of Fermi level values. V_{Li}^- corresponds to removing a Li^+ ion from pristine $LiNH_2$, and Li_i^+ corresponds to adding a Li^+ ion in the space between two NH_2^- units. We find that these defects lead to structural relaxations corresponding to slight displacements and rotations of the neighboring Li^+ and NH_2^- units. For the hydrogen-related defects, V_H^- corresponds to removing an H^+ ion from pristine $LiNH_2$ to result in an NH^{2-} unit. The formation of H_i^+ leads to a neutral NH_3 unit, which is an NH_2^- unit with an extra H^+ ion.

In the absence of electrically active impurities, or when such impurities occur in much lower concentrations than charged native defects, the Fermi level position is determined by oppositely charged defects with the lowest formation energies.[8,9] According to Figure 1, these are Li_i^+ and V_{Li}^-, thus fixing the Fermi level at $\varepsilon_F = 2.49$ eV. At this Fermi level value, the calculated formation energy of Li_i^+ and V_{Li}^- is 0.51 eV, while the formation energies of H_i^+ and V_H^- are 1.28 and 0.63 eV, respectively.

The activation energy of a process that involves native defects depends not only on the defect formation energies but also on the migration barriers. We find migration barriers of 0.61 and 0.71 eV for H_i^+ and V_H^-, respectively, by using the climbing-image elastic band method.[10] For H_i^+, an H^+ ion in the NH_3 unit moves to the nearest NH_2^- unit; the saddle-point configuration consists of an H^+ ion located midway between two NH_2^- units. Migration of V_H^- involves moving an H^+ ion from a nearby NH_2^- unit to the vacancy, that is, the NH^{2-} unit; the saddle-point configuration in this case consists of a H^+ ion located midway between two NH^{2-} units. For the lithium-related defects, the migration of Li_i^+ involves moving the Li^+ ion from one ground-state interstitial site to another, with a migration barrier as low as 0.30 eV. For V_{Li}^-, a Li^+ ion moves from a nearby lattice site to the vacancy with a migration barrier of 0.20 eV. These values indicate that Li_i^+ and V_{Li}^- are highly mobile even at temperatures below room temperature, thus implying that lithium-related defects readily achieve equilibrium concentrations at the temperatures of interest for decomposition.

We also investigated the formation of lithium and hydrogen Frenkel pairs. Figure 2 shows the structure of a (H_i^+, V_H^-) pair. The configurations of the individual defects are preserved in this complex; that is, H_i^+ forms an NH_3 unit and V_H^-

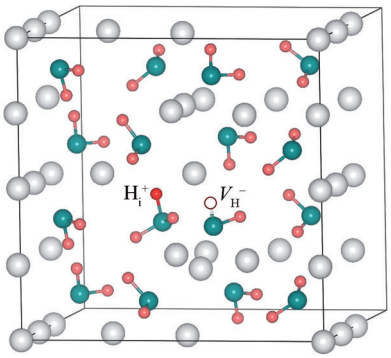

Figure 2. Structure of the (H_i^+, V_H^-) Frenkel pair. H red, Li gray, N blue. The removed H atom of V_H^- is represented by an empty sphere.

forms an adjacent NH^{2-} unit. This hydrogen-related Frenkel pair has a formation energy of 1.54 eV and a binding energy of 0.38 eV (with respect to the isolated constituents). The distance between the two N ions in the pair is 3.37 Å, which is very close to the N–N distance in pristine $LiNH_2$ (3.38 Å). The lithium-related Frenkel pair (Li_i^+, V_{Li}^-) has a formation energy of 0.65 eV and a binding energy of 0.36 eV; the distance between Li_i^+ and V_{Li}^- is 0.85 Å. Note that our calculated formation energy for (Li_i^+, V_{Li}^-) is lower than the value of 0.97 eV reported by Miceli et al.[11] The formation energy is low (much lower than that of the hydrogen-related Frenkel pair), thus indicating that $LiNH_2$ is prone to Frenkel disorder on the Li sublattice.

The transformation of $LiNH_2$ into Li_2NH, such as in Equation (2), necessitates the breaking of N–H bonds, thus indicating that not only lithium-related but also hydrogen-related defects are required. In particular, V_H^- must be formed, either in the interior of the material or at the surface. The creation of V_H^- in the interior of $LiNH_2$ is necessarily accompanied by the creation of H_i^+, so that mass and charge are conserved. In contrast, V_H^- can be created at the surface by the removal of an H^+ ion from $LiNH_2$, with the resulting H^+ accommodated as an adsorbed atom or reacting with nearby species. These two possibilities, namely formation of V_H^- in the interior of $LiNH_2$ or at the surface, can be regarded as two different mechanisms for the reaction. The mechanism that predominates will depend on the relative number of reaction sites available. Since one mechanism involves atoms in the bulk and the other involves atoms at the surface, the mechanism will depend on the surface-to-volume ratio. As discussed below, the two mechanisms have different activation energies, thus leading to the experimentally observed dependence of activation energies on the SSA. We now describe the mechanisms in more detail:

Mechanism 1: (H_i^+, V_H^-) Frenkel pairs are created in the interior of $LiNH_2$ by moving an H^+ ion from a lattice site to an interstitial site (see Figure 2). Next, V_H^- and H_i^+ are separated as H_i^+ jumps from one NH_2^- unit to another. This process is

equivalent to displacing the NH_3 unit away from the NH^{2-} unit, and leaves two Li^+ ions next to the NH^{2-} unit; that is, a formula unit of Li_2NH is locally formed inside $LiNH_2$. The H_i^+ ion migrates to the surface and is released as NH_3. We assume that as the H_i^+ ion migrates from one NH_2^- unit to the next, a corresponding Li_i^+ moves in the opposite direction (with a very low activation energy), thus maintaining local charge neutrality. The overall activation energy for this mechanism is 2.52 eV, which is equal to the formation energies of H_i^+ and V_H^- plus the migration barrier of H_i^+.

Mechanism 2: V_H^- is created at the surface by removing an H^+ ion from $LiNH_2$. This H^+ ion can combine with a surface NH_2^- unit to form NH_3 that is subsequently released. The rate-limiting step in this mechanism is not the formation of V_H^- at the surface, but the hydrogen mass transport to the surface; that is, in order to maintain this reaction, H^+ ions have to be transported to the surface (equivalent to V_H^- diffusing into the interior). In this case, the activation energy is 1.34 eV for hydrogen self-diffusion mediated by V_H^-, that is, the sum of its formation energy and migration barrier. The Li^+ ion that is left after a surface NH_2^- unit combines with an H^+ ion and is released in the form of NH_3, assists the self-diffusion of V_H^-, as required by the charge neutrality condition.

In $LiNH_2$ samples subjected to ball milling, the activation energy for decomposition decreases with milling time, from 2.53 eV (before ball milling, SSA: 3.72 $m^2 g^{-1}$) to 1.43 eV (after 3 h of milling, SSA: 46.65 $m^2 g^{-1}$).[2] In samples composed of sufficiently large $LiNH_2$ particles, the surface-to-volume ratio is small and mechanism 1 (which depends on creation of defects in the bulk) prevails. Our calculated activation energy of 2.52 eV is in very good agreement with the experimental value of 2.53 eV for the activation energy for decomposition of $LiNH_2$ before ball milling.[2] In samples composed of relatively small particles, on the other hand, the surface-to-volume ratio is large and mechanism 2 prevails. The calculated activation energy of 1.34 eV is again in good agreement with experimentally determined activation energies for the decomposition of ball-milled $LiNH_2$, which range from 1.33 to 1.43 eV.[2,12] As the milling time increases, the particle size decreases, and we expect the activation energy to decrease smoothly as the SSA decreases. Note that in both mechanisms, the highly mobile V_{Li}^- and Li_i^+ defects, which also have low formation energies, serve to provide local charge neutrality and assist mass transport.

Our proposed mechanisms can also explain the dehydrogenation of ($LiNH_2$+LiH) mixtures [Eq. (1)]. It is expected that $LiNH_2$ and LiH are in intimate contact if the reactants are carefully mixed. At the $LiNH_2$/LiH interface, LiH provides Li^+ and H^- ions, for example, by forming Schottky defects in LiH. These species can diffuse into $LiNH_2$ and/or react with the corresponding units at the $LiNH_2$ surface. H^- ions can combine with H_i^+ to form H_2 without releasing any NH_3. H_i^+ is either created in the bulk of $LiNH_2$ and transported to the $LiNH_2$/LiH interface by mechanism 1; or, alternatively, an H^+ ion is liberated from $LiNH_2$ when creating V_H^- by mechanism 2. On the other hand, Li^+ ions can migrate across the $LiNH_2$/LiH interface and assist in forming Li_2NH. This behavior explains the formation of Li_2NH and H_2 in Equation (1). If $LiNH_2$ and LiH are not in intimate contact, NH_3 may be produced according to Equation (2) because the H^- ions (from LiH) are not immediately available to combine with H^+ ions before the latter is released from $LiNH_2$ in the form of NH_3. In this case, the resulting NH_3 can be captured by LiH according to Equation (3) and/or released as one of the products.

It has been experimentally shown that the activation energy for the dehydrogenation of ($LiNH_2$+LiH) mixtures also decreases with increasing ball-milling time.[3,4] Shaw et al. reported activation energies of 1.70 eV (before ball milling, SSA: 4.65 $m^2 g^{-1}$), 1.36 eV (after 1.5 h, SSA: 47.36 $m^2 g^{-1}$), 1.18 eV (after 3 h, SSA: 51.32 $m^2 g^{-1}$), and 0.65 eV (after 24 h, SSA: 62.35 $m^2 g^{-1}$) for the dehydrogenation of ($LiNH_2$+LiH) mixtures.[3] Varin et al., on the other hand, reported a different set of activation energies: 2.46 eV (before ball milling, SSA: 16.5 $m^2 g^{-1}$), 0.98 eV (after 1 h, SSA: 26.4 $m^2 g^{-1}$), 0.88 eV (after 25 h, SSA: 59.6 $m^2 g^{-1}$), and 0.91 eV (after 100 h, SSA: 45.6 $m^2 g^{-1}$).[4] Both sets of data show similar trends: the activation energy is reduced significantly with ball milling and there is a correlation with the measured SSA.

The trend in the experimental activation energies is again consistent with our proposed explanation in terms of a bulk- versus surface-dominated mechanism for the decomposition of $LiNH_2$. For those samples that exhibit activation energies lower than that in mechanism 2 (1.34 eV), we suggest that the milling process may have created a high-energy state in the ($LiNH_2$+LiH) mixtures, in which defect concentrations are well above the equilibrium concentrations; the activation energy is then lowered because the energy cost of forming the rate-limiting defects no longer needs to be paid, thus leaving only the migration energy cost. In this case, the activation energy would be as low as 0.71 eV, that is, the migration barrier of V_H^-.

In summary, we have proposed specific atomistic mechanisms for the decomposition of $LiNH_2$ that explain the particle-size dependence of the activation energy for decomposition. While our present study is devoted to understanding $LiNH_2$ decomposition, our approach is not limited to $LiNH_2$ but can be applied to other hydrogen storage systems.

Methods

Calculations were based on ab initio density functional theory within the generalized-gradient approximation[13] and the projector augmented wave method,[14,15] as implemented in the VASP code.[16–18] For defect calculations in $LiNH_2$ (tetragonal; 32 atoms per unit cell),[19] we used a ($2\times2\times1$) supercell which contains 128 atoms, a $2\times2\times2$ Monkhorst–Pack k-point mesh,[20] and plane-wave basis-set cutoff of 400 eV. Migration barriers were studied using the climbing-image nudged elastic band method.[10]

The formation energy of a defect X in charge state q is defined as[21]

$$E^f(X^q) = E_{tot}(X^q) - E_{tot}(\text{bulk}) - \sum_i n_i\mu_i + q(E_v + \Delta V + \varepsilon_F), \quad (4)$$

where $E_{tot}(X^q)$ and E_{tot}(bulk) are the total energies of a supercell containing defect X and of a supercell of the perfect bulk material, respectively; μ_i is the atomic chemical potential of species i

(referenced to the standard state), and n_i denotes the number of atoms of species i that have been added ($n_i > 0$) or removed ($n_i < 0$) to form the defect. ε_F is the electron chemical potential, that is, the Fermi level, referenced to the VBM in the bulk (E_v). ΔV is the "potential alignment" term, that is, the shift in the band positions that arises from the presence of the charged defect, obtained by aligning the average electrostatic potential in regions far away from the defect to the bulk value.[21]

The chemical potentials μ_{Li}, μ_N, and μ_H are variables and can be chosen to represent experimental conditions. Given the reported transformation between $LiNH_2$ and Li_2NH,[7] it is reasonable to assume that the two compounds are in contact. The temperature and pressure values at which the decomposition process occurs determine μ_H through equilibrium with H_2 gas. In this work, we employ a set of conditions used by David et al. for hydrogen desorption, namely 10^{-3} bar and 260 °C.[7] A different set of chemical potentials corresponding to different experimental conditions can of course be chosen, and this may affect the relative defect formation energies. We have verified, however, that the details of this choice do not affect the physics of the mechanisms presented here.

Received: January 31, 2011
Revised: June 16, 2011
Published online: July 5, 2011

Keywords: amides · dehydrogenation · hydrogen storage · kinetics · nanoparticles

[1] P. Chen, Z. T. Xiong, J. Z. Luo, J. Y. Lin, K. L. Tan, *Nature* **2002**, *420*, 302 – 304.
[2] T. Markmaitree, R. Ren, L. L. Shaw, *J. Phys. Chem. B* **2006**, *110*, 20710 – 20718.
[3] L. L. Shaw, R. Ren, T. Markmaitree, W. Osborn, *J. Alloys Compd.* **2008**, *448*, 263 – 271.
[4] R. A. Varin, M. Jang, M. Polanski, *J. Alloys Compd.* **2010**, *491*, 658 – 667.
[5] Y. H. Yu, E. Ruckenstein, *J. Phys. Chem. A* **2003**, *107*, 9737 – 9739.
[6] T. Ichikawa, N. Hanada, S. Isobe, H. Leng, H. Fujii, *J. Phys. Chem. B* **2004**, *108*, 7887 – 7892.
[7] W. I. F. David, M. O. Jones, D. H. Gregory, C. M. Jewell, S. R. Johnson. A. Walton, P. P. Edwards, *J. Am. Chem. Soc.* **2007**, *129*, 1594 – 1601.
[8] A. Peles, C. G. Van de Walle, *Phys. Rev. B* **2007**, *76*, 214101.
[9] G. B. Wilson-Short, A. Janotti, K. Hoang, A. Peles, C. G. Van de Walle, *Phys. Rev. B* **2009**, *80*, 224102.
[10] G. Henkelman, B. P. Uberuaga, H. Jónsson, *J. Chem. Phys.* **2000**, *113*, 9901 – 9904.
[11] G. Miceli, C. S. Cucinotta, M. Bernasconi, M. Parrinello, *J. Phys. Chem. C* **2010**, *114*, 15174 – 15183.
[12] P. E. Pinkerton, *J. Alloys Compd.* **2005**, *400*, 76 – 82.
[13] J. P. Perdew, K. Burke, M. Ernzerhof, *Phys. Rev. Lett.* **1996**, *77*, 3865 – 3868.
[14] P. E. Blöchl, *Phys. Rev. B* **1994**, *50*, 17953 – 17979.
[15] G. Kresse, D. Joubert, *Phys. Rev. B* **1999**, *59*, 1758 – 1775.
[16] G. Kresse, J. Hafner, *Phys. Rev. B* **1993**, *47*, 558 – 561.
[17] G. Kresse, J. Furthmüller, *Phys. Rev. B* **1996**, *54*, 11169 – 11186.
[18] G. Kresse, J. Furthmüller, *Comput. Mater. Sci.* **1996**, *6*, 15 – 50.
[19] J. B. Yang, X. D. Zhou, Q. Cai, W. J. James, W. B. Yelon, *Appl. Phys. Lett.* **2006**, *88*, 041914.
[20] H. J. Monkhorst, J. D. Pack, *Phys. Rev. B* **1976**, *13*, 5188 – 5192.
[21] C. G. Van de Walle, J. Neugebauer, *J. Appl. Phys.* **2004**, *95*, 3851 – 3879.

